Viscosity and dilepton production of a chemically equilibrating quark-gluon plasma at finite baryon density

Nana Guan,[1,2] Zejun He,[1,*] Jiali Long,[1] Xiangzhou Cai,[1] Yugang Ma,[1] Jianwei Li,[1,2] and Wenqing Shen[1]

[1]*Shanghai Institute of Applied Physics, Chinese Academy of Sciences, Shanghai 201800, People's Republic of China*

[2]*Graduate School of the Chinese Academy of Sciences, Beijing 100080, People's Republic of China*

(Received 17 February 2009; revised manuscript received 9 June 2009; published 24 July 2009)

By considering the effect of shear viscosity we have investigated the evolution of a chemically equilibrating quark-gluon plasma at finite baryon density. Based on the evolution of the system we have performed a complete calculation for the dilepton production from the following processes: $q\bar{q}\to l\bar{l}$, $q\bar{q}\to gl\bar{l}$, Compton-like scattering ($qg\to ql\bar{l}$, $\bar{q}g\to\bar{q}l\bar{l}$), gluon fusion ($g\bar{g}\to c\bar{c}$), annihilation ($q\bar{q}\to c\bar{c}$), as well as the multiple scattering of quarks. We have found that quark-antiquark annihilation, Compton-like scatterring, gluon fusion, and multiple scattering of quarks give important contributions. Moreover, we have also found that the dilepton yield is an increasing function of the initial quark chemical potential, and the increase of the quark phase lifetime because of the viscosity also obviously raises the dilepton yield.

DOI: 10.1103/PhysRevC.80.014908 PACS number(s): 12.38.Mh, 25.75.−q, 24.10.Nz

I. INTRODUCTION

The Relativistic Heavy-Ion Collider (RHIC) at the Brookhaven National Laboratory and the Large Hadron Collider (LHC) being built at CERN will provide the best opportunity to study the formation and evolution of quark-gluon plasma (QGP). Dileptons have large mean free paths owing to the small cross section for electromagnetic interaction in the plasma; they therefore can provide an ideal probe for the detection and study of the plasma.

Many authors [1–3], by considering the created QGP in collisions to be a thermodynamic equilibrium system, have studied dilepton production. Recently, photon and dilepton production was studied based on the evolution model of chemically equilibrating QGP, established by Shuryak, Biró, and co-workers [4–6], and studies of their production in plasma at finite baryon density were also performed [7,8]. However, in most previous work the partonic plasma was assumed to be ideal (i.e., without any viscous effect). In principle, viscous effects in fluid hydrodynamics should not be neglected in a realistic scenario since the dimension of the plasma is comparable to the mean free path of the partons. The viscous coefficient in the framework of hydrodynamics is composed of bulk and shear viscosity, but the bulk viscosity vanishes for a quark-gluon plasma [9]. In this work, we mainly discuss the effect of the shear viscosity, which have attracted many authors to investigate its influences on the formation and evolution of the QGP system. The authors of Ref. [9] have studied the viscous corrections to the hydrodynamic equations describing the evolution of the QGP at finite baryon density and investigated the effect of viscosity on chemical equilibration of the system. They have found that because of the viscosity the lifetime of the plasma increases, the temperature evolution of the system becomes slower, and the chemical equilibration of the system becomes faster, thereby increasing the reaction rate. However, we should point out that in previous work many authors have regarded the viscous coefficients as adjustable parameters [9–12]. Indeed, they should be directly obtained from the thermodynamic quantities of the system. However, the viscous coefficients derived by Danielewicz and Gyulassy [13] based on QCD phenomenology for a baryon-free plasma and by Hou and Li [14] considering Debye screening and the damping rate of gluons for a baryon-rich plasma using finite-temperature QCD are so large that the temperature of the plasma would be abnormally raised.

In early calculations, one mainly considered the dilepton production from the process $q\bar{q}\to l\bar{l}$. In recent years, possible sources of dileptons, such as $q\bar{q}\to l\bar{l}$ annihilation, $qg\to ql\bar{l}$ Compton-like scattering, and $qg\to qgl\bar{l}$ fusion, were investigated [15,16]. In addition, the contributions of gluon fusion ($gg\to c\bar{c}$), quark-antiquark annihilation ($q\bar{q}\to c\bar{c}$), and multiple scattering of quarks to dileptons have also been studied [17].

In this work, starting from the shear viscous coefficient given by relativistic kinetic theory for a massless QGP under the relaxation time approximation, we first estimate the mean free paths of partons in a chemically equilibrating QGP at finite baryon density, then combined with the parton energy densities, we calculate the shear viscous coefficient of the QGP. Subsequently, based on our evolution model including the viscosity, we perform a complete calculation for the dilepton production from the processes $q\bar{q}\to l\bar{l}$, $q\bar{q}\to gl\bar{l}$, Compton-like scattering ($qg\to ql\bar{l}$, $\bar{q}g\to\bar{q}l\bar{l}$), gluon fusion ($g\bar{g}\to c\bar{c}$), annihilation ($q\bar{q}\to c\bar{c}$), as well as multiple scattering of quarks, to predict the contributions of these reaction processes and reveal the effect of the finite baryon density and viscous phenomena on dilepton production.

The rest of the paper is organized as follows: Sec. II describes the evolution of the dissipative QGP system. In Sec. III, we discuss the yields of dileptons of the system. We give our results and present a discussion in Sec. IV. Finally, in Sec. V, we offer a brief summary and conclusions.

*hezejun@sinap.ac.cn

II. EVOLUTION OF THE DISSIPATIVE QGP SYSTEM

In this work, we describe the distribution functions of partons with Jüttner distributions $f_{q(\bar{q})} = \lambda_{q(\bar{q})}/(e^{(p\mp\mu_q)/T} + \lambda_{q(\bar{q})})$ for quarks (antiquarks) and $f_g = \lambda_g/(e^{p/T} - \lambda_g)$ for gluons, where fugacity $\lambda_i(\leqslant 1)$ of the parton of type i is used to characterize the nonequilibrium of the system. Based on these distribution functions, we first derive the thermodynamic relations of the chemically equilibrating QGP system at finite baryon density. Expanding densities of quarks (antiquarks),

$$n_{q(\bar{q})} = \frac{g_{q(\bar{q})}}{2\pi^2}\lambda_{q(\bar{q})}\int \frac{p^2 dp}{\lambda_{q(\bar{q})} + e^{(p\mp\mu_q)/T}}, \tag{1}$$

over quark chemical potential μ_q, we get the baryon density of the system [18],

$$\begin{aligned} n_{b,q} = \frac{g_q}{6\pi^2}\Big[&T^3\big(Q_1^2\lambda_q - \bar{Q}_1^2\lambda_{\bar{q}}\big) + 2\mu_q T^2\big(Q_1^1\lambda_q + \bar{Q}_1^1\lambda_{\bar{q}}\big) \\ &+ T\mu_q^2\big(Q_1^0\lambda_q - \bar{Q}_1^0\lambda_{\bar{q}}\big) + \frac{1}{3}\mu_q^3\left(\frac{\lambda_q}{\lambda_q+1} + \frac{\lambda_{\bar{q}}}{\lambda_{\bar{q}}+1}\right)\Big] \end{aligned} \tag{2}$$

and the corresponding energy density

$$\begin{aligned} \epsilon_{\rm QGP} = \frac{g_q}{2\pi^2}\Big[&T^4\big(Q_1^3\lambda_q + \bar{Q}_1^3\lambda_{\bar{q}}\big) + 3\mu_q T^3\big(Q_1^2\lambda_q - \bar{Q}_1^2\lambda_{\bar{q}}\big) \\ &+ 3\mu_q^2 T^2\big(Q_1^1\lambda_q + \bar{Q}_1^1\lambda_{\bar{q}}\big) + T\mu_q^3\big(Q_1^0\lambda_q - \bar{Q}_1^0\lambda_{\bar{q}}\big) \\ &+ \frac{1}{4}\mu_q^4\left(\frac{\lambda_q}{\lambda_q+1} + \frac{\lambda_{\bar{q}}}{\lambda_{\bar{q}}+1}\right) \\ &+ \frac{g_g}{g_q}T^4 G_1^3\lambda_g + \frac{2\pi^2 B_0}{g_q}\Big], \end{aligned} \tag{3}$$

where $g_{q(\bar{q})}$ and g_g are degeneracy factors of quarks (antiquarks) and gluons, respectively. Since the convergence of the integral factors

$$\begin{aligned} G_m^n &= \int \frac{Z^n dZ}{(e^Z - \lambda_g)^m}, \quad Q_m^n = \int \frac{Z^n dZ}{(e^Z + \lambda_q)^m}, \\ \bar{Q}_m^n &= \int \frac{Z^n dZ}{(e^Z + \lambda_{\bar{q}})^m} \end{aligned} \tag{4}$$

appearing in the expansion is very rapid, it is easy to calculate these integrals numerically [18].

We consider the reactions leading to chemical equilibrium: $gg \rightleftharpoons ggg$ and $gg \rightleftharpoons q\bar{q}$. By assuming that elastic parton scatterings are sufficiently rapid to maintain local thermal equilibrium, the evolutions of gluon and quark densities can be given by the master equations, respectively. We first extend the master equations to include the viscosity as done in Ref. [9]. Similarly, the evolution of baryon density can be described by a corrected conservation equation of baryon number including a viscous term. In addition, because of viscosity, a viscous term would be contained in the conservation equation of the energy-momentum, too. Combining the master equations together with the equation of baryon number conservation and equation of energy-momentum conservation including viscous corrections, for longitudinal scaling expansion of the system, one can get a set of coupled relaxation equations (CRE) describing the evolution of the temperature T, quark chemical potential μ_q, and fugacities λ_q for quarks and λ_g for gluons on the basis of the thermodynamic relations of the chemically equilibrating QGP system at finite baryon density [9,18]:

$$\begin{aligned} &\left(\frac{1}{\lambda_g} + \frac{G_2^2}{G_1^2}\right)\dot{\lambda_g} + 3\frac{\dot{T}}{T} + \frac{1}{\tau} = R_3\left[1 - \frac{G_1^2}{2\xi(3)}\lambda_g\right] \\ &\quad - 2R_2\left[1 - \left(\frac{2\xi(3)}{G_1^2}\right)^2 \frac{n_g n_{\bar{q}}}{\bar{n_g}\bar{n_{\bar{q}}}}\frac{1}{\lambda_g^2}\right] + \frac{\eta}{\epsilon\tau^2}, \end{aligned} \tag{5}$$

$$\begin{aligned} &\dot{\lambda_q}\Big[T^3\big(Q_1^2 - \lambda_q Q_2^2\big) + 2\mu_q T^2\big(Q_1^1 - \lambda_q Q_2^1\big) \\ &\quad + T\mu_q^2\big(Q_1^0 - \lambda_q Q_2^0\big) + \frac{1}{3}\mu_q^3\frac{1}{(\lambda_q+1)^2}\Big] \\ &\quad + \dot{T}\big[3\lambda_q T^2 Q_1^2 + 4\lambda_q\mu_q T Q_1^1 + \lambda_q\mu_q^2 Q_1^0\big] \\ &\quad + \dot{\mu_q}\left[2\lambda_q T^2 Q_1^1 + 2\lambda_q\mu_q T Q_1^0 + \mu_q^2\frac{\lambda_q}{\lambda_q+1}\right] + \frac{n_q^0}{\tau} \\ &= n_g^0 R_2\left[1 - \left(\frac{2\xi(3)}{G_1^2}\right)^2 \frac{1}{\lambda_g^2}\frac{n_g n_{\bar{q}}}{\bar{n_g}\bar{n_{\bar{q}}}}\frac{1}{\lambda_g^2}\right] + \frac{\eta n_q^0}{\epsilon\tau^2}, \end{aligned} \tag{6}$$

$$\begin{aligned} &\dot{\lambda_q}\left[2T^2\mu_q\big(Q_1^1 - \lambda_q Q_2^1\big) + \frac{1}{3}\mu_q^3\frac{1}{(\lambda_q+1)^2}\right] \\ &\quad + \dot{T}4\lambda_q\mu_q T Q_1^1 + \dot{\mu_q}\left[2\lambda_q T^2 Q_1^1 + \mu_q^2\frac{\lambda_q}{\lambda_q+1}\right] \\ &= -\frac{1}{\tau}\left[2T^2\mu_q Q_1^1\lambda_q + \frac{1}{3}\mu_q^3\frac{\lambda_q}{\lambda_q+1}\right] + \frac{6\pi^2}{g_q}\frac{\eta n_b}{\epsilon\tau^2}, \end{aligned} \tag{7}$$

$$\begin{aligned} &\dot{\lambda_g}\frac{g_g}{g_q}T^4\big(G_1^3 + \lambda_g G_2^3\big) + \dot{\lambda_q}\Big[2T^4\big(Q_1^3 - \lambda_q Q_2^3\big) \\ &\quad + 6T^2\mu_q^2\big(Q_1^1 - \lambda_q Q_2^1\big) + \frac{1}{2}\mu_q^4\frac{1}{(\lambda_q+1)^2}\Big] \\ &\quad + \dot{T}\left[8\lambda_q T^3 Q_1^3 + 12\lambda_q\mu_q^2 T Q_1^1 + 4\frac{g_g}{g_q}\lambda_g T^3 G_1^3\right] \\ &\quad + \dot{\mu_q}\left[12\mu_q\lambda_q T^2 Q_1^1 + 2\mu_q^3\frac{\lambda_q}{\lambda_q+1}\right] \\ &= -\frac{4}{3\tau}\Big[2T^4 Q_1^3\lambda_q + 6T^2\mu_q^2\lambda_q Q_1^1 + \frac{\mu_q^4}{2}\frac{\lambda_q}{\lambda_q+1} \\ &\quad + \frac{g_g}{g_q}\lambda_q T^4 G_1^3\Big] + \frac{4}{3}\frac{2\pi^2}{g_q}\frac{\eta}{\tau^2}, \end{aligned} \tag{8}$$

where $\bar{n}_{q(\bar{q})}$ is the value of $n_{q(\bar{q})}$ at $\lambda_{q(\bar{q})} = 1$, $n_q^0 = n_q/(g_q/2\pi^2)$, $n_g^0 = n_g/(g_g/2\pi^2)$, $\xi(3) = 1.20206$, and η is the shear viscous coefficient. The gluon and quark production rates R_3/T and R_2/T are, respectively, given by [6,18–20]

$$R_3/T = \frac{32}{3a_1}\frac{\alpha_s}{\lambda_g}\left[\frac{(M_D^2 + s/4)M_D^2}{9g^2T^4/2}\right]^2 I(\lambda_g, \lambda_q, T, \mu_q), \tag{9}$$

$$R_2/T = \frac{g_g}{24\pi}\frac{G_1^{12}}{G_1^2}N_f\alpha_s^2\lambda_g\ln\left(\frac{1.65}{\alpha_s\lambda_g}\right), \tag{10}$$

$$M_D^2 = \frac{3g^2T^2}{\pi^2}\left[2G_1^1\lambda_g + 2N_f Q_1^1\lambda_q + N_f\left(\frac{\mu_q}{T}\right)^2\left(\frac{\lambda_q}{\lambda_q+1}\right)\right], \quad (11)$$

where M_D^2 is the Debye screening mass, $g^2 = 4\pi\alpha_s$, and $I(\lambda_g, \lambda_q, T, \mu_q)$ is the function of λ_g, λ_q, T, and μ_q, as used in Refs. [5,6]. We here take the quark flavor $N_f = 2.5$ [8,19,20]. Solving the set of evolution equations (5)–(8) under given initial values obtained from the Hijing model, we can obtain the evolution of temperature T, quark chemical potential μ_q, and fugacities λ_q for quarks and λ_g for gluons.

To discuss the effects of the shear viscous coefficient, we have quoted two different expressions of it. The coefficients η_1 and η_2 are taken from Refs. [9,13], respectively:

$$\eta_1 = \eta_0\frac{\epsilon_{\rm QGP}}{T}, \quad (12)$$

$$\eta_2 = \frac{T}{\sigma_\eta}\left[\frac{n_g}{\frac{9}{4}n_g + n_q} + \frac{n_q}{\frac{4}{9}n_q + n_g}\right], \quad (13)$$

where η_0 is treated as a constant [9] and σ_η is the transport cross section [13].

Now, we discuss the calculation of the viscous coefficient η in our work. According to Refs. [13,14,21], the shear viscous coefficient using the relativistic kinetic theory for a massless QGP in the relaxation time approximation is written as

$$\eta_i = \tfrac{4}{15}\epsilon_i\lambda_i, \quad (14)$$

where λ_i is the mean free path of particle of type i in QGP, which in a chemically equilibrating QGP for the gluon is given by

$$\lambda_g = \frac{4}{9n_g}\frac{1}{2\pi{\alpha_s}^2}\frac{M_D^2\left(M_D^2 + 9T^2/2\right)}{9T^2/2} \quad (15)$$

and for quark by

$$\lambda_q = \frac{9}{4n_q}\frac{1}{2\pi{\alpha_s}^2}\frac{M_D^2\left(M_D^2 + 9T^2/2\right)}{9T^2/2}, \quad (16)$$

where M_D^2 is the Debye screening mass, which is given by Eq. (11). Thus, we can directly calculate the viscous coefficients η_g and η_q and their total η from the thermodynamic quantities of the QGP system.

III. DILEPTON PRODUCTION

Based on the evolution of the QGP system, we first consider dilepton production from quark annihilation $q\bar{q}\to gl\bar{l}$ and Compton scatterings $qg\to ql\bar{l}$ and $\bar{q}g\to\bar{q}l\bar{l}$. Their production rates can be calculated by [16]

$$E\frac{dR}{d^3p} = \frac{1}{2(2\pi)^8}\int\frac{d^3p_1}{2E_1}\frac{d^3p_2}{2E_2}\frac{d^3p_3}{2E_3}f_1(E_1)f_2(E_2) \times[1\pm f_3(E_3)]\cdot\delta^4(P_1+P_2-P_3-K)\sum|M|^2, \quad (17)$$

where $f(E)$ is the Jüttner distribution function of partons and $\sum|M|^2$ is the square of the matrix element for reaction processes summed over spins, colors, and flavors. The plus sign is for the annihilation process and the minus sign for the two Compton processes. According to Ref. [22], these equation can be rewritten as

$$\frac{dR}{d^2M} = \frac{100}{27}\frac{\alpha^2\alpha_s}{\pi^5M}\int dsdt\frac{u^2+t^2+2sM^2}{ut}\lambda_q^2 \times\int\frac{dE_1}{e^{(E_1-\mu_q)/T}+\lambda_q}\frac{dE_2}{e^{(E_1+\mu_q)/T}+\lambda_q}\int\frac{dE}{E} \times\left[1+\frac{\lambda_g}{e^{(E_1+E_2-E)/T}-\lambda_g}\right]\frac{\theta[P(E_1,E_2)]}{[P(E_1,E_2)]^{1/2}} \quad (18)$$

for the annihilation process and

$$\frac{dR}{d^2M} = 20\frac{\alpha^2\alpha_s}{\pi^5M}\int dsdt\frac{u^2+s^2+2tM^2}{-us}\lambda_q\lambda_g \times\int\frac{dE_1}{e^{(E_1\mp\mu_q)/T}+\lambda_q}\frac{dE_2}{e^{(E_1)/T}-\lambda_g}\int\frac{dE}{E} \times\left[1-\frac{\lambda_q}{e^{(E_1+E_2-E\mp\mu_q)/T}+\lambda_q}\right]\frac{\theta[P(E_1,E_2)]}{[P(E_1,E_2)]^{1/2}} \quad (19)$$

for Compton scattering, where $P(E_1,E_2) = -[tE_1+(s+t)E_2]^2 + 2Es[(s+t)E_2 - tE_1] - s^2E^2 + s^2t + st^2$, θ is the step function, α is the fine-structure constant, and α_s is the running coupling constant. The minus sign is for the Compton process $qg\to ql\bar{l}$ and the plus sign for $\bar{q}g\to\bar{q}l\bar{l}$. The letters s, t, and u are the Mandelstam variables. The integrations are performed over $-(s-M^2)+k_c^2\leqslant t\leqslant -k_c^2$ and $M^2+2k_c^2\leqslant s<\infty$ [16]. The cutoff k_c^2 is replaced by the thermal quark mass $2m_q^2$ [22]. For a chemically equilibrating QGP system at finite baryon density m_q^2 is given by

$$m_q^2 = \frac{4\alpha_s}{3\pi}T^2\left[2\left(G_1^1\lambda_g + Q_1^1\lambda_q\right) + \left(\frac{\mu_q}{T}\right)^2\frac{\lambda_q}{\lambda_q+1}\right], \quad (20)$$

where integral factors G_1^1 and Q_1^1 have been given in the previous section.

Obviously, these calculations give up the infrared contribution because of the introduction of the infrared cutoff k_c^2. The authors of Ref. [22] have discussed the infrared contribution to photon production. Following their calculation, in this work, we have given an assessment of the contribution from the infrared part to the dilepton produnction. The dilepton production rate with total energy E and total momentum $\mathbf{p}$ can be calculated by [22,23]

$$\frac{dR}{dEd^3p} = \frac{\alpha}{12\pi^4}\frac{1}{P^2}\frac{1}{e^{E/T}-1}{\rm Im}\Pi^\mu_{R,\mu}, \quad (21)$$

where $\Pi_R^{\mu\nu}$ is the retarded photon self-energy. The infrared divergence mentioned here is caused by propagation of soft momenta. To resolve the problem it is necessary to dress one of the quark propagators (as done in Fig. 3 of Ref. [22]). Then

the retarded photon self-energy can be written as [22]

$$\Pi^{\mu\nu}(p) = -\frac{5}{3}e^2T\sum_{k_0}\int\frac{d^3k}{(2\pi)^3}\mathrm{Tr}[S^*(k)\gamma^\mu S(p-k)\gamma^\nu], \quad (22)$$

where $S^*(k)$ is the dressed propagator for a quark with four-momentum k and $S(q)$ is the bara propagator for a quark with four-momentum $q = p - k$. Following Ref. [22], after performing some calculations and applying the elegant method developed by Braaten, Pisarski, and Yuan [23], one can finally obtain a simplified expression of the imaginary part of the retarded photon self-energy,

$$\mathrm{Im}\Pi^\mu_{R,\mu} = \frac{5e^2}{6\pi}(e^{E/T}-1)\int_0^{k_c}dk\int_{-k}^{k}d\omega f(\omega)f(E-\omega) \times(k-\omega)\beta_+(\omega,k), \quad (23)$$

where f is the Jüttner distribution function of partons and

$$\beta_+(\omega,k) = \frac{\frac{1}{2}m_q^2(k-\omega)}{\left\{k(\omega-k)-m_q^2[Q_0(z)-Q_1(z)]\right\}^2+\left[\frac{1}{2}\pi m_q^2(1-z)\right]^2}, \quad (24)$$

where $z = \omega/k$ [24] and Q_0 and Q_1 are the Legendre functions of the second kind. After integrating over the dilepton energy ($E \geqslant M$) one can obtain the dilepton production rate over the square invariant mass of dileptons, dR/dM^2.

Similar to the preceding treatment, the production rate of quark-antiquark annihilation $q\bar{q}\to l\bar{l}$ can be given by [25]

$$\frac{dR}{dM^2} = \frac{5}{24\pi^4}M^2\sigma_{l\bar{l}}(M^2) \times\int_0^\infty dp_1 f_q(p_1)\int_{M^2/4p_1}^\infty dp_2 f_q(p_2), \quad (25)$$

where $\sigma_{l\bar{l}}(M^2) = \frac{20}{3}4\pi\alpha^2/3M^2$ is the quark annihilation cross section.

Aurenche, Gelis, and their co-workers have studied dilepton production from bremsstrahlung and off-shell annihilation where the quark undergoes multiple scattering in the medium, as shown in Fig. 1 of Ref. [26]. Their calculation includes the Landau-Pomeranchuk-Migdal effect and they concluded that this contribution is important. According to these authors' approach, the imaginary part of the retarded current-current correlator $\Pi^\mu_{R,\mu}(P)$ in Eq. (21) can be computed by

$$\mathrm{Im}\Pi^\mu_{R,\mu} \approx \frac{5}{6\pi}\int_{-\infty}^{+\infty}dq_0[f(k_0)-f(q_0)] \times\mathrm{Re}\int\frac{d^2\boldsymbol{q}_\perp}{(2\pi)^2}\left[\frac{q_0^2+k_0^2}{2(q_0k_0)^2}\boldsymbol{q}_\perp\cdot\boldsymbol{f}(\boldsymbol{q}_\perp) + \frac{1}{\sqrt{|q_0k_0|}}\frac{P^2}{p^2}g(\boldsymbol{q}_\perp)\right], \quad (26)$$

where $k_0 \equiv q_0 + E$, f is the Jüttner distribution function of partons again, and the dimensionless functions $\boldsymbol{f}(\boldsymbol{q}_\perp)$ and $g(\boldsymbol{q}_\perp)$, respectively, obey the integral equations [26]

$$2\boldsymbol{q}_\perp = i\delta E\boldsymbol{f}(\boldsymbol{q}_\perp) + \frac{4}{3}g_s^2T\int\frac{d^2\boldsymbol{l}_\perp}{(2\pi)^2}\mathcal{C}(\boldsymbol{l}_\perp) \times[\boldsymbol{f}(\boldsymbol{q}_\perp)-\boldsymbol{f}(\boldsymbol{q}_\perp+\boldsymbol{l}_\perp)] \quad (27)$$

and

$$2\sqrt{|q_0k_0|} = i\delta Eg(\boldsymbol{q}_\perp) + g_s^2C_FT\int\frac{d^2\boldsymbol{l}_\perp}{(2\pi)^2}\mathcal{C}(\boldsymbol{l}_\perp) \times[g(\boldsymbol{q}_\perp)-g(\boldsymbol{q}_\perp+\boldsymbol{l}_\perp)]. \quad (28)$$

Using the method described in Ref. [26], we recast Eqs. (27) and (28) as differential equations and solve them using a simple algorithm, finally, getting $\mathrm{Re}\int d^2\boldsymbol{q}_\perp/(2\pi)^2\boldsymbol{q}_\perp\cdot\boldsymbol{f}(\boldsymbol{q}_\perp)$ and $\mathrm{Re}\int d^2\boldsymbol{q}_\perp/(2\pi)^2 g(\boldsymbol{q}_\perp)$ and the corresponding dilepton production rate of the multiple scattering process.

For the QGP system, produced in collisions at RHIC energies, with very high initial temperature (≈0.57 GeV) [6,18], thermal charmed quark production and its contribution to lepton pairs should be contained, especially, those from the gluon fusion $gg\to c\bar{c}$ and quark-antiquark annihilation $q\bar{q}\to c\bar{c}$. Similar to the calculation for $q\bar{q}\to l\bar{l}$, by replacing the cross section $\sigma_{l\bar{l}}(M^2)$ appearing in Eq. (25) with those of the reactions $q\bar{q}\to c\bar{c}$ and $gg\to c\bar{c}$ in leading order QCD, we can compute the yields of charm pairs in the QGP. Almost all of the produced thermal charmed quarks would eventually hadronize to D mesons [17]. By considering that the D meson decays to leptons with a 17% branching ratio for charged D mesons [17,27,28], one can obtain the contribution of charmed quarks from reactions $gg\to c\bar{c}$ and $q\bar{q}\to c\bar{c}$ to lepton pairs.

We integrate these production rates over the space-time volume of the reaction. According to Bjorken's model, the volume element is $d^4x = d^2x_T dy\tau d\tau$, where τ is the evolution time of the system and y is the rapidity of the fluid element. We consider $Au^{197} + Au^{197}$ central collisions, so the integration over transverse coordinates just yields a factor of $d^2x_T = \pi R_A^2$, where R_A is the nuclear radius. Finally, we obtain the dilepton spectra of the system,

$$\frac{dN}{dydM^2} = \pi R_A^2\int\tau d\tau\frac{dR}{dM^2}. \quad (29)$$

IV. CALCULATED RESULTS AND DISCUSSION

In this work, we focus on discussing $Au^{197} + Au^{197}$ central collisions at RHIC energies. To compare with Refs. [9,29,30], we take initial values of the system from the Hijing model calculation: $\tau_0 = 0.70$ fm, $T_0 = 0.570$ GeV, $\lambda_{g0} = 0.08$, and $\lambda_{q0} = 0.02$. We have investigated the effect of viscosity on the evolution of the system using those expressions of the shear viscosity as shown in Eqs. (12)–(16). To understand the effect of the baryon density on the dilepton production, we have solved the CRE for initial quark chemical potentials $\mu_{q0} = 0.000$, 0.284, 0.568, and 0.852 GeV for given viscous coefficients and obtained the evolution of the temperature T, quark chemical potential μ_q, and fugacities λ_g and λ_q of the system. In Fig. 1, we show the evolution of the temperature T with proper time τ for the various viscous coefficients from the expressions in Refs. [9,13]. Following Ref. [9], we

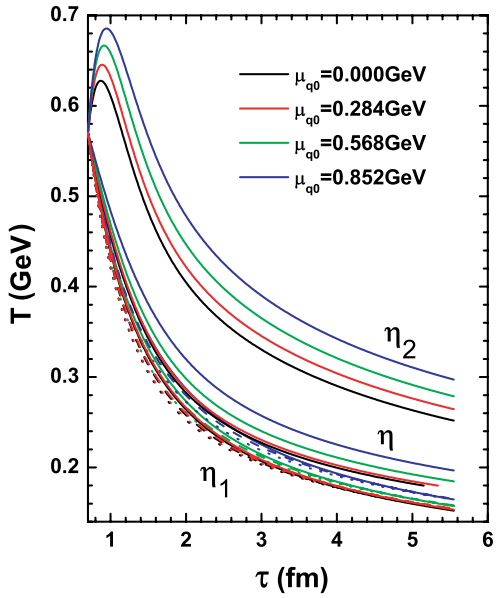

FIG. 1. (Color online) The evolution of the temperature T with proper time τ for viscous coefficients η_1, η_2, and η at initial quark chemical potentials $\mu_{q0} = 0.000$, 0.284, 0.568, and 0.852 GeV. η_1 is the viscous coefficient for parameters $\eta_0 = 0.0$, 0.4, and 0.8 as given in Ref. [9], and the corresponding values are denoted by the solid, dashed, and dotted curves, respectively.

take the parameters $\eta_0 = 0.0$, 0.4, and 0.8. The corresponding curves are indicated by the solid, dashed, and dotted lines, respectively. We can see that the viscosity leads to an increase of the temperature of the QGP system. We also note that the temperature is unreasonably raised for viscous coefficient η_2. For η_1, the evolution of temperature seems to be reasonable; however, the viscosity η_1 is only obtained through adjusting the parameter η_0. In this work, we have calculated the viscous coefficients η by the thermodynamic quantities of the QGP system using Eqs. (14)–(16). From Fig. 1, we note that the calculated temperature distribution is reasonable. In addition, the temperature is also an increasing function of the initial quark chemical potential. Figure 2 shows the value of η as a function of the initial temperature, where the black, red, green, and blue curves denote, in turn, the calculated η for initial quark chemical potentials $\mu_{q0} = 0.000$, 0.284, 0.568, and 0.852 GeV at the initial values previously mentioned. From Fig. 2, one can see that η increases with increasing temperature T.

The estimated evolution paths of the system in the phase diagram are shown in Fig. 3, where black, red, green, and blue curves are, in turn, the calculated evolution paths for initial quark chemical potentials $\mu_{q0} = 0.000$, 0.284, 0.568, and 0.852 GeV. The solid line is the phase boundary between the quark phase and hadronic phase. The lines with open circles denote the evolution of the system without viscosity; the lines with solid circles are from the system with viscosity. The time interval between the two circles is 0.3 fm. The corresponding equilibration rates of gluons and quarks, λ_g and λ_q, are shown in Fig. 4. The solid lines are for the cases of viscosity and the short dashed lines denote ideal cases, where the black, red, green, and blue curves are, in turn, the calculated values for

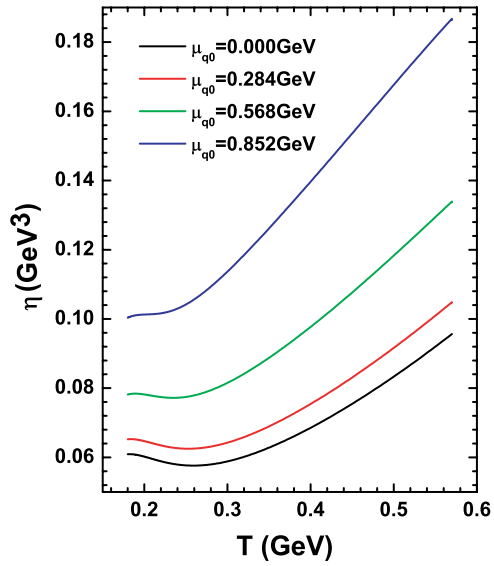

FIG. 2. (Color online) The viscous coefficient η as a function of the temperature. Black, red, green, and blue denote, in turn, the calculated viscous coefficients η for initial quark chemical potentials $\mu_{q0} = 0.000$, 0.284, 0.568, and 0.852 GeV at the same initial conditions as given in Fig. 1.

initial quark chemical potentials $\mu_{q0} = 0.000$, 0.284, 0.568, and 0.852 GeV. From Figs. 3 and 4 we see that the evolution of the system becomes slower owing to viscosity, whereas the equilibration rate of the plasma becomes faster compared to the one in the ideal case. Also, the effect of the initial quark chemical potential on the evolution is in accordance with the previous conclusion of Ref. [18].

Based on the evolution of the system described in Figs. 3 and 4, we have calculated dilepton spectra for processes $q\bar{q} \to l\bar{l}$, $q\bar{q} \to gl\bar{l}$, $qg \to ql\bar{l}$, $\bar{q}g \to \bar{q}l\bar{l}$, $q\bar{q} \to c\bar{c}$, $gg \to c\bar{c}$, and multiple scattering at the four initial quark chemical potentials

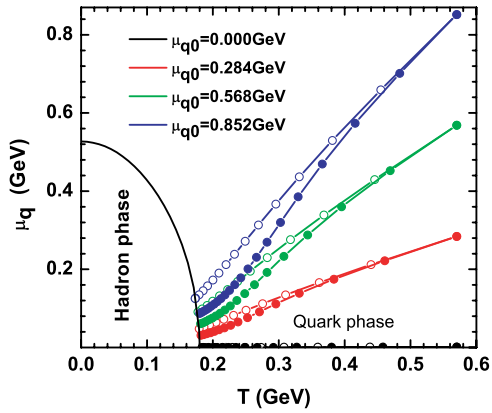

FIG. 3. (Color online) The calculated evolution paths of the system in the phase diagram for the initial values as given in Fig. 1, where black, red, green and blue curves are, in turn, the calculated evolution paths for initial quark chemical potentials $\mu_{q0} = 0.000$, 0.284, 0.568, and 0.852 GeV. The lines with open circles denote the evolution of the system without viscous effect; the lines with solid circles are the evolution of the system with viscosity. The time interval between the two circles is 0.3 fm.

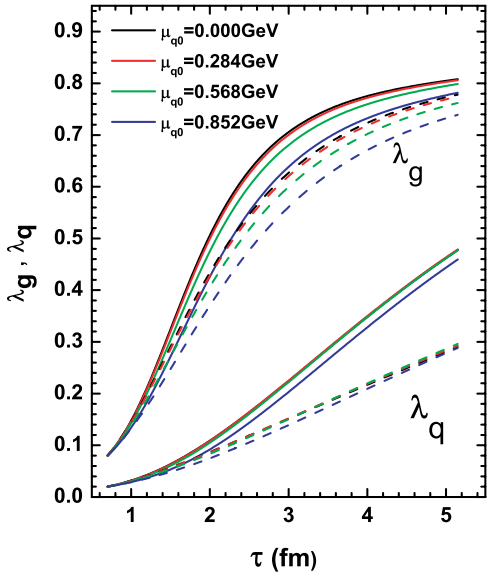

FIG. 4. (Color online) The calculated equilibration rates at the same initial conditions as given in Fig. 1. The solid lines are for the cases of viscosity and the dashed lines are for the ideal cases, where the black, red, green, and blue lines are the calculated values for initial quark chemical potentials $\mu_{q0} = 0.000, 0.284, 0.568$, and 0.852 GeV.

as previously given. The calculated dilepton spectra from quark annihilation processes $q\bar{q} \to l\bar{l}$ and $q\bar{q} \to gl\bar{l}$ are, in turn, shown in Figs. 5(a) and 5(b). The solid lines are the spectra of the system with the effect of viscosity and the dashed

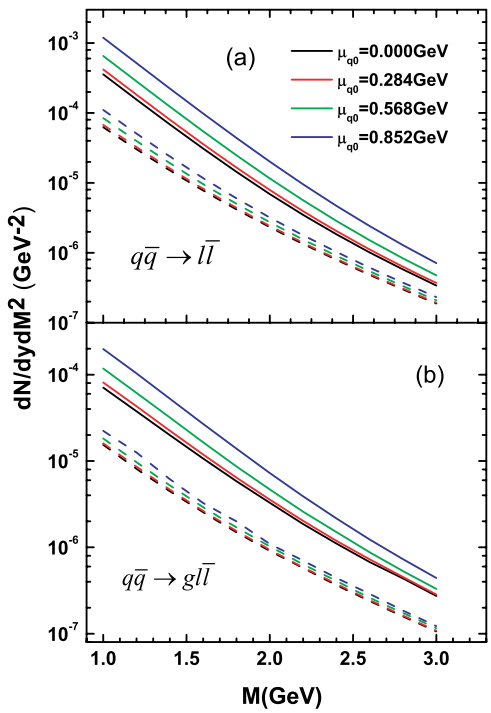

FIG. 5. (Color online) The calculated dilepton spectra from quark annihilation processes $q\bar{q} \to l\bar{l}$ and $q\bar{q} \to gl\bar{l}$. The curves have the same meaning as those in Fig. 4.

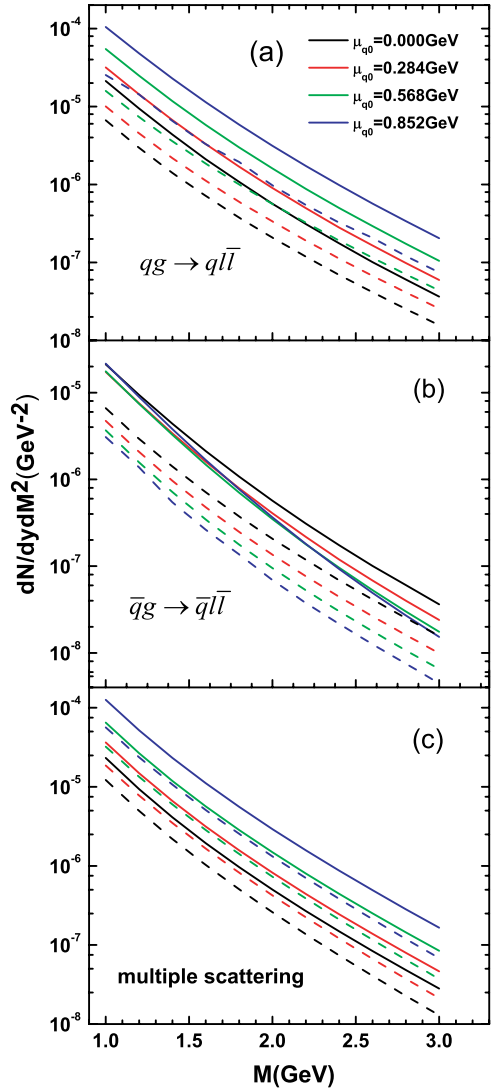

FIG. 6. (Color online) The calculated dilepton spectra from processes $qg \to ql\bar{l}$ and $\bar{q}g \to \bar{q}l\bar{l}$ and multiple scattering. The curves have the same meaning as those in Figs. 4 and 5.

lines indicate those from the ideal system, where the black, red, green, and blue lines denote the calculated spectra for initial quark chemical potentials $\mu_{q0} = 0.000, 0.284, 0.568$, and 0.852 GeV. One can see that the calculated spectrum goes up with increasing initial quark chemical potential. The law is valid for processes $qg \to ql\bar{l}$ and multiple scattering as shown in Figs. 6(a) and 6(c). We know that the quark density goes up with the increase of quark chemical potential whereas the antiquark density goes down, which will lead to a suppression of the production from the process $\bar{q}g \to \bar{q}l\bar{l}$, as shown in Fig. 6(b). We can also see from Figs. 5 and 6 that the dilepton production is an increasing function of viscosity, which would be mainly attributable to the increase of the quark phase lifetime because of the viscosity.

The production of soft dileptons, which are connected with the infrared contribution, has been computed following

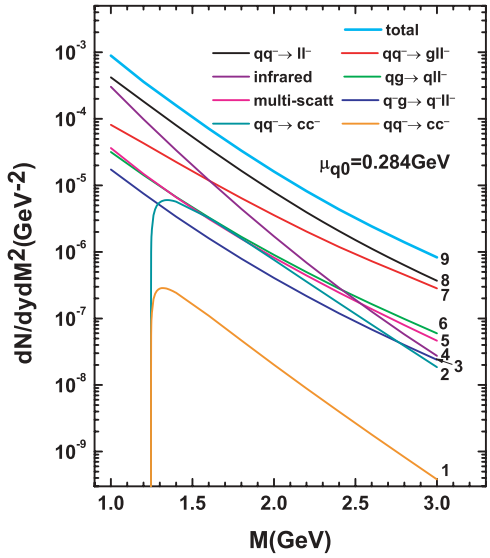

FIG. 7. (Color online) The calculated spectra of all processes for the initial quark chemical potential $\mu_{q0} = 0.284$ GeV. Curves 1–9 are, in turn, the calculated spectra for $q\bar{q} \to c\bar{c}$, $gg \to c\bar{c}$, $\bar{q}g \to \bar{q}l\bar{l}$, soft dileptons, multiple scattering, $qg \to ql\bar{l}$, $q\bar{q} \to gl\bar{l}$, $q\bar{q} \to l\bar{l}$, and their total.

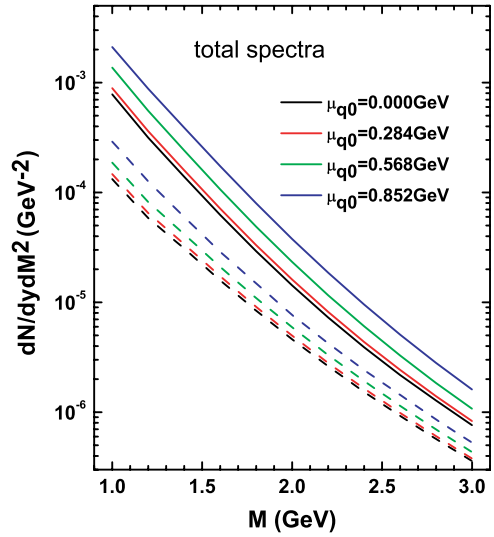

FIG. 8. (Color online) The calculated total dilepton spectra of the system. The curves have the same meaning as those in previous figures.

the method represented in Ref. [23] for initial quark chemical potentials $\mu_{q0} = 0.000, 0.284, 0.568$, and 0.852 GeV. In Fig. 7 we show the results from all processes and their total for the initial quark chemical potential $\mu_{q0} = 0.284$ GeV. Curves 1–9 represent, in turn, the calculated spectra for $q\bar{q} \to c\bar{c}$, $gg \to c\bar{c}$, $\bar{q}g \to \bar{q}l\bar{l}$, soft dileptons, multiple scattering, $qg \to ql\bar{l}$, $q\bar{q} \to gl\bar{l}$, $q\bar{q} \to l\bar{l}$, and their total. From Fig. 7, one can see that the spectra from the quark-antiquark annihilations $q\bar{q} \to l\bar{l}$ and $q\bar{q} \to gl\bar{l}$ dominate. The infrared contribution is as important as that of reaction $q\bar{q} \to gl\bar{l}$ and even higher than the later one in the range of small invariant mass. The contributions from Compton-like scattering $qg \to ql\bar{l}$, multiple scattering, and annihilation $gg \to c\bar{c}$ cannot also be neglected.

We have also given the total yields of all processes of the system for initial conditions previously mentioned, as shown in Fig. 8. The black, red, green, and blue curves represent the total yields for $\mu_{q0} = 0.000, 0.284, 0.568$, and 0.852 GeV, respectively. To understand the effect of viscosity on the dilepton production, we also give the yields for the ideal QGP system, which are denoted by dashed lines. It shows clearly that the dilepton yield of the system goes up with increasing initial quark chemical potential. However, previous authors have found that dileptons produced in a thermodynamic equilibrium QGP system are suppressed with increasing initial quark chemical potential [1]. In this work, since both the quark chemical potential and the temperature of the system are functions of time, compared with the baryon-free QGP it necessarily takes a long time for the value (μ_q, T) of the system to reach a certain point of the phase boundary to make the phase transition. Furthermore, in the calculation we have found that with increasing initial quark chemical potential the production rate of gluons goes up, and thus their equilibration rate goes down, leading to a small energy consumption of the system (i.e., a slow cooling of the system). Since there are many more gluons than quarks in the system, increasing the initial quark chemical potential further slows down the cooling of the system. These cause the quark phase lifetime to further increase, as seen in Fig. 3. These effects will raise the dilepton yield and compensate the dilepton suppression, leading the spectrum of the system to be an increasing function of the initial quark chemical potential. However, as seen in Fig. 3, because of the viscosity the evolution of the system becomes even slower, so that the dilepton yield will be raised, as seen in Fig. 8. From Fig. 8 one can note that the dilepton yields are remarkably raised by the effect of the viscosity of the QGP system.

V. SUMMARY AND CONCLUSION

In this work, by taking into account reactions $gg \rightleftharpoons ggg$ and $gg \rightleftharpoons q\bar{q}$ leading to the chemical equilibrium of the QGP system and conservations of energy-momentum and baryon number, as well as viscosity of the QGP system, we have derived a set of coupled CRE of the chemically equilibrating QGP system with viscosity at finite baryon density, produced from $Au^{197} + Au^{197}$ central collisions at RHIC energies, which describes the space-time evolution of the system. Then, we have solved the CRE and directly obtained the viscous coefficients from the thermodynamic quantities of the QGP system. We note that the calculated results of the viscous coefficients are reasonable. Subsequently, based on the evolution of the QGP system we have computed the dilepton spectra of the QGP system, finding that the spectra are dominated by the quark-antiquark annihilation $q\bar{q} \to l\bar{l}$ and $q\bar{q} \to gl\bar{l}$, followed by the multiple scattering of quarks, compton-like scattering $qg \to ql\bar{l}$, and annihilation $gg \to c\bar{c}$. We have also calculated the infrared contribution and found it to be very important at the range of small invariant mass of dileptons. Furthermore, we note that the increase of the

dilepton yield with increasing initial quark chemical potential can compensate for the dilepton suppression, thus eventually leading to the dilepton spectrum to be an increasing function of the initial quark chemical potential. Especially, we have found that the dilepton yield of the system is obviously enhanced by the viscous effect because this effect slows the evolution of the system and thus the lifetime of the QGP system increases.

ACKNOWLEDGMENTS

This work is supported in part by the Knowledge Innovation Project of the Chinese Academy of Science under Grant No. KJCX2-N11, CAS master scholar fund, the National Natural Science Foundation of China under Grant Nos. 10075071, 10605037, and 10875159, and the Major State Basic Research Development Program in China under Contract No. G200077400.

[1] A. Dumitru, D. H. Rischke, T. Schonfeld, L. Winckelmann, H. Stöcker, and W. Greiner, Phys. Rev. Lett. **70**, 2860 (1993).
[2] J. Sollfrank, P. Huovinen, M. Kataja, P. V. Ruuskanen, M. Prakash, and R. Venugopalan, Phys. Rev. C **55**, 392 (1997).
[3] Z. J. He *et al.*, Phys. Lett. **B495**, 317 (2000).
[4] E. Shuryak, Phys. Rev. Lett. **68**, 3270 (1992).
[5] K. J. Eskola and X. N. Wang, Phys. Rev. D **49**, 1284 (1994).
[6] T. S. Bíró, E. van Doorn, B. Müller, M. H. Thoma, and X. N. Wang, Phys. Rev. C **48**, 1275 (1993).
[7] D. Dutta, K. Kumar, A. K. Mohanty, and R. K. Choudhury, Phys. Rev. C **60**, 014905 (1999).
[8] A. Majumder and C. Gale, Phys. Rev. D **63**, 114008 (2001).
[9] D. Dutta, A. K. Mohanty, K. Kumar, and R. K. Choudhury, Phys. Rev. C **61**, 034902 (2000).
[10] T. S. Bíró, E. Molnár, and P. Ván, Phys. Rev. C **78**, 014909 (2008).
[11] H. Song and U. Heinz, Phys. Rev. C **78**, 024902 (2008).
[12] A. Muronga, Phys. Rev. C **76**, 014909 (2007).
[13] P. Danielewicz and M. Gyulassy, Phys. Rev. D **31**, 53 (1985).
[14] D. Hou and J. Li, Nucl. Phys. **A618**, 371 (1997).
[15] B. Kämpfer *et al.*, Z. Phys. A **353**, 71 (1995).
[16] B. Kämpfer, O. P. Pavlenko, A. Peshier, and G. Soff, Phys. Rev. C **52**, 2704 (1995).
[17] A. Shor, Phys. Lett. **B233**, 231 (1989).
[18] Z. J. He, J. L. Long, W. Z. Jiang, Y. G. Ma, and B. Liu, Phys. Rev. C **68**, 024902 (2003).
[19] C. T. Traxler and M. H. Thoma, Phys. Rev. C **53**, 1348 (1996).
[20] P. Levai, B. Müller, and X. N. Wang, Phys. Rev. C **51**, 3326 (1995).
[21] M. H. Thoma, Phys. Rev. D **49**, 451 (1994).
[22] J. Kapusta, P. Lichard, and D. Seibert, Phys. Rev. D **44**, 2774 (1991).
[23] E. Braaten, R. D. Pisarski, and T. C. Yuan, Phys. Rev. Lett. **64**, 2242 (1990).
[24] V. V. Klimov, Sov. J. Nucl. Phys. **33**, 934 (1981).
[25] M. Strickland, Phys. Lett. **B331**, 245 (1994).
[26] P. Aurenche, F. Gelis, G. D. Moore, and H. Zaraket, J. High Energy Phys. 12 (2002) 006.
[27] B. L. Combridge, Nucl. Phys. **B151**, 429 (1979).
[28] R. M. Baltrusaitis *et al.*, Phys. Rev. Lett. **54**, 1976 (1985).
[29] D. Pal, A. Sen, M. G. Mustafa, and D. K. Srivastava, Phys. Rev. C **65**, 034901 (2002).
[30] P. Levai and X. N. Wang, AIP Conf. Proc. **340**, 363 (1995).